Spectrometer

As already pointed out above, there is a difference between medium-resolution spectrometers that are used for LS AAS and high-resolution spectrometers that are designed for CS AAS. The spectrometer includes the spectral sorting device (monochromator) and the detector.

Spectrometers for LS AAS

In LS AAS the high resolution that is required for the measurement of atomic absorption is provided by the narrow line emission of the radiation source, and the monochromator simply has to resolve the analytical line from other radiation emitted by the lamp. This can usually be accomplished with a band pass between 0.2 and 2 nm, i.e., a medium-resolution monochromator. Another feature to make LS AAS element-specific is modulation of the primary radiation and the

use of a selective amplifier that is tuned to the same modulation frequency, as already postulated by Alan Walsh. This way any (unmodulated) radiation emitted for example by the atomizer can be excluded, which is imperative for LS AAS. Simple monochromators of the Littrow or (better) the Czerny-Turner design are typically used for LS AAS. Photomultiplier tubes are the most frequently used detectors in LS AAS, although solid state detectors might be preferred because of their better signal-to-noise ratio.

Spectrometers for CS AAS

When a continuum radiation source is used for AAS measurement it is indispensable to work with a high-resolution monochromator. The resolution has to be equal to or better than the half width of an atomic absorption line (about 2 pm) in order to avoid losses of sensitivity and linearity of the calibration graph. The research with high-resolution (HR) CS AAS was pioneered by the groups of O'Haver and Harnly in the USA, who also developed the (up until now) only simultaneous multi-element spectrometer for this technique. The break-through, however, came when the group of Becker-Ross in Berlin, Germany, built a spectrometer entirely designed for HR-CS AAS. The first commercial equipment for HR-CS AAS was introduced by Analytik Jena (Jena, Germany) at the beginning of the 21st century, based on the design proposed by Becker-Ross and Florek. These spectrometers use a compact double monochromator with a prism pre-monochromator and an echelle grating monochromator for high resolution. A linear charge coupled device (CCD) array with 200 pixels is used as the detector. The second monochromator does not have an exit slit; hence the spectral environment at both sides of the analytical line becomes visible at high resolution. As typically only 3–5 pixels are used to measure the atomic absorption, the other pixels are available for correction purposes. One of these corrections is that for lamp flicker noise, which is independent of wavelength, resulting in measurements with very low noise level; other corrections are those for background absorption, as will be discussed later.

Background absorption and background correction

The relatively small number of atomic absorption lines (compared to atomic emission lines) and their narrow width (a few pm) make spectral overlap rare; there are only very few examples known that an absorption line from one element will overlap with another. Molecular absorption, in contrast, is much broader, so that it is more likely that some molecular absorption band will overlap with an atomic line. This kind of absorption might be caused by un-dissociated molecules of concomitant elements of the sample or by flame gases. We have to distinguish between the spectra of di-atomic molecules, which exhibit a pronounced fine structure, and those of larger (usually tri-atomic) molecules that don't show such fine structure. Another source of background absorption, particularly in ET AAS, is scattering of the primary radiation at particles that are generated in the atomization stage, when the matrix could not be removed sufficiently in the pyrolysis stage.

All these phenomena, molecular absorption and radiation scattering, can result in artificially high absorption and an improperly high (erroneous) calculation for the concentration or mass of the analyte in the sample. There are several techniques available to correct for background absorption, and they are significantly different for LS AAS and HR-CS AAS.

Background correction techniques in LS AAS

In LS AAS background absorption can only be corrected using instrumental techniques, and all of them are based on two sequential measurements, firstly, total absorption (atomic plus background), secondly, background absorption only, and the difference of the two measurements gives the net atomic absorption. Because of this, and because of the use of additional devices in the spectrometer, the signal-to-noise ratio of background-corrected signals is always significantly inferior compared to uncorrected signals. It should also be pointed out that in LS AAS there is no way to correct for (the rare case of) a direct overlap of two atomic lines. In essence there are three techniques used for background correction in LS AAS:

Deuterium background correction

This is the oldest and still most commonly used technique, particularly for flame AAS. In this case, a separate source (a deuterium lamp) with broad emission is used to measure the background absorption over the entire width of the exit slit of the spectrometer. The use of a separate lamp makes this technique the least accurate one, as it cannot correct for any structured background. It also cannot be used at wavelengths above about 320 nm, as the emission intensity of the deuterium lamp becomes very weak. The use of deuterium HCL is preferable compared to an arc lamp due to the better fit of the image of the former lamp with that of the analyte HCL.

Smith-Hieftje background correction

This technique (named after their inventors) is based on the line-broadening and self-reversal of emission lines from HCL when high current is applied. Total absorption is measured with normal lamp current, i.e., with a narrow emission line, and background absorption after application of a high-current pulse with the profile of the self-reversed line, which has little emission at the original wavelength, but strong emission on both sides of the analytical line. The advantage of this technique is that only one radiation source is used; among the disadvantages are that the high-current pulses reduce lamp lifetime, and that the technique can only be used for relatively volatile elements, as only those exhibit sufficient self-reversal to avoid dramatic loss of sensitivity. Another problem is that background is not measured at the same wavelength as total absorption, making the technique unsuitable for correcting structured background.

Zeeman-effect background correction

An alternating magnetic field is applied at the atomizer (graphite furnace) to split the absorption line into three components, the π component, which remains at the same position as the original absorption line, and two σ components, which are moved to higher and lower wavelengths, respectively (see Zeeman Effect). Total absorption is measured without magnetic field and background absorption with the magnetic field on. The π component has to be removed in this case, e.g. using a polarizer, and the σ components do not overlap with the emission profile of the lamp, so that only the background absorption is measured. The advantages of this technique are

1. that total and background absorption are measured with the same emission profile of the same lamp, so that any kind of background, including background with fine structure can be corrected accurately, unless the molecule responsible for the background is also affected by the magnetic field

2. using a chopper as a polariser reduces the signal to noise ratio. While the disadvantages are the increased complexity of the spectrometer and power supply needed for running the powerful magnet needed to split the absorption line.

Background correction techniques in HR-CS AAS

In HR-CS AAS background correction is carried out mathematically in the software using information from detector pixels that are not used for measuring atomic absorption; hence, in contrast to LS AAS, no additional components are required for background correction.

Background correction using correction pixels

It has already been mentioned that in HR-CS AAS lamp flicker noise is eliminated using correction pixels. In fact, any increase or decrease in radiation intensity that is observed to the same extent at all pixels chosen for correction is eliminated by the correction algorithm. This obviously also includes a reduction of the measured intensity due to radiation scattering or molecular absorption, which is corrected in the same way. As measurement of total and background absorption, and correction for the latter, are strictly simultaneous (in contrast to LS AAS), even the fastest changes of background absorption, as they may be observed in ET AAS, do not cause any problem. In addition, as the same algorithm is used for background correction and elimination of lamp noise, the background corrected signals show a much better signal-to-noise ratio compared to the uncorrected signals, which is also in contrast to LS AAS.

Background correction using a least-squares algorithm

The above technique can obviously not correct for a background with fine structure, as in this case the absorbance will be different at each of the correction pixels. In this case HR-CS AAS is offering the possibility to measure correction spectra of the molecule(s) that is (are) responsible for the background and store them in the computer. These spectra are then multiplied with a factor to match the intensity of the sample spectrum and subtracted pixel by pixel and spectrum by spectrum from the sample spectrum using a least-squares algorithm. This might sound complex, but first of all the number of di-atomic molecules that can exist at the temperatures of the atomizers used in AAS is relatively small, and second, the correction is performed by the computer within a few seconds. The same algorithm can actually also be used to correct for direct line overlap of two atomic absorption lines, making HR-CS AAS the only AAS technique that can correct for this kind of spectral interference.

RAMAN SPECTROSCOPY

Raman spectroscopy is a form of vibrational spectroscopy, much like infrared (IR) spectroscopy. However, whereas IR bands arise from a change in the dipole moment of a molecule due to an interaction of light with the molecule, Raman bands arise from a change in the polarizability of the molecule due to the same interaction. This means that these observed bands (corresponding to specific energy transitions) arise from specific molecular vibrations. When the energies of these transitions are plotted as a spectrum, they can be used to identify the molecule as they provide a "molecular fingerprint" of the molecule being observed. Certain vibrations that are allowed in Raman are forbidden in IR, whereas other vibrations may be observed by both techniques although at significantly different intensities thus these techniques can be thought of as complementary.

Since the discovery of the Raman effect in 1928 by C.V. Raman and K.S. Krishnan, Raman spectroscopy has become an established as well as a practical method of chemical analysis & characterization applicable to many different chemical species.

Samples may be in the form of

- Solids (particles, pellets, powers, films, fibers)
- Liquids (gels, pastes)
- Gases

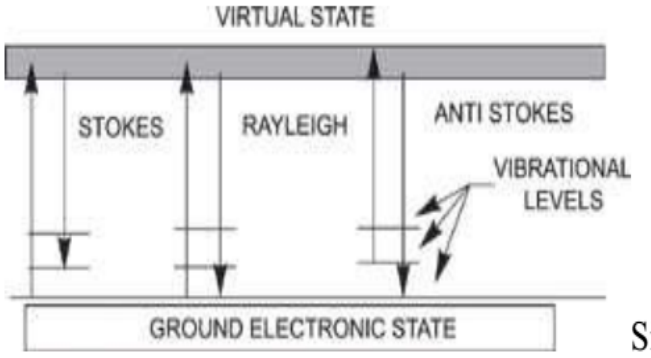

Simplified energy diagram

It is the shift in wavelength of the inelastically scattered radiation that provides the chemical and structural information. Raman shifted photons can be of either higher or lower energy, depending upon the vibrational state of the molecule under study. A simplified energy diagram that illustrates these concepts is shown on the right.

Stokes radiation occurs at lower energy (longer wavelength) than the Rayleigh radiation, and anti-Stokes radiation has greater energy. The energy increase or decrease is related to the vibrational energy levels in the ground electronic state of the molecule, and as such, the observed Raman shift of the Stokes and anti-Stokes features are a direct measure of the vibrational energies of the molecule. A schematic Raman spectrum may appear as shown below.

The energy of the scattered radiation is less than the incident radiation for the Stokes line and the energy of the scattered radiation is more than the incident radiation for the anti-Stokes line. The energy increase or decrease from the excitation is related to the vibrational energy spacing in the ground electronic state of the molecule and therefore the wavenumber of the Stokes and anti-Stokes lines are a direct measure of the vibrational energies of the molecule.

In the example spectrum, notice that the Stokes and anti-Stokes lines are equally displaced from the Rayleigh line. This occurs because in either case one vibrational quantum of energy is gained or lost. Also, note that the anti-Stokes line is much less intense than the Stokes line. This occurs because only molecules that are vibrationally excited prior to irradiation can give rise to the anti-Stokes line. Hence, in Raman spectroscopy, only the more intense Stokes line is normally measuredRaman scattering is a relatively weak process. The number of photons Raman scattered is quite small. However, there are several process which can be used to enhance the sensitivity of a Raman measurement.

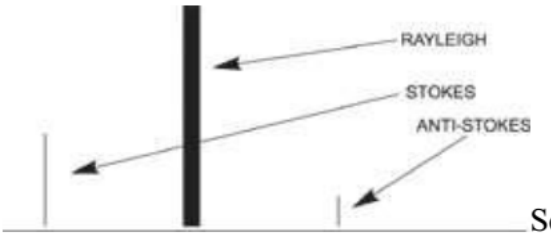

Schematic Raman spectrum

If the wavelength of the exciting laser coincides with an electronic absorption of a molecule, the intensity of Raman- active vibrations associated with the absorbing chromophore are enhanced by a factor of 102 to 104. This resonance enhancement or resonance Raman effect can be extremely useful, not just in significantly lowering the detection limits, but also in introducing electronic selectivety. Thus the resonance Raman technique is used for providing both structural and electronic insight into species of interest. Metalloporphyrins, carotenoids and several other classes of biologically important molecules have strongly allowed electronic transitions in the visible, making them ideal candidates for resonance Raman spectroscopy.Resonance selectivity has a further practical use, in that spectrum of the chromophoric moiety is resonance enhanced and that of the surrounding environment is not. For biological chromophores, this means that absorbing active centres can be specifically probed by visible excitation wavelengths, and not the surrounding protein matrix (which would require UV lasers to bring into resonance). Resonance Raman spectroscopy is also an important probe of the chemistry of metal centred complexes, fullerenes, polydiacetylenes and other "exotic" molecules which strongly absorb in the visible. Although many more molecules absorb in the ultraviolet, the high cost of lasers and optics for this spectral region have limited ultraviolet (UV) resonance Raman spectroscopy to a small number of specialist groups.

Vibrations which are resonantly enhanced fall into two or three general mechanistic classes. The most common case is Franck-Condon enhancement, in which a component of the normal coordinate of the vibration occurs in a direction in which the molecule expands during an electronic excitation. The more the molecule expands along this axis when it absorbs light, the larger the enhancement factor. The easily visualized ring breathing (in-plane expansion) modes of porphyrins fall into this class.Vibrations which couple two electronic excited states are also resonantly enhanced, through a mechanism called vibronic enhancement. In both cases, enhancement factors roughly follow the intensities of the absorption spectrum. The fuller theory of resonance enhancement is beyond the scope of this section.

Resonance enhancement does not begin at a sharply defined wavelength. In fact, enhancement of 5x to 10x is observed if the exciting laser is within even a few 100 wavenumbers below the electronic transition of a molecule. This "pre-resonance" enhancement can be experimentally useful.

The Raman scattering from a compound (or ion) adsorbed on or even within a few Angstroms of a structured metal surface can be 103 to 106x greater than in solution. This surface-enhanced Raman scattering is strongest on silver, but is observable on gold and copper as well. At practical excitation wavelengths, enhancement on other metals is unimportant. SERS arises from two mechanisms:

• The first is an enhanced electromagnetic field produced at the surface of the metal. When the wavelength of the incident light is close to the plasma wavelength of the metal, conduction electrons in the metal surface are excited into an extended surface electronic excited state called a surface plasmon resonance. Molecules adsorbed or in close proximity to the surface experience an exceptionally large electromagnetic field. Vibrational modes normal to the surface are most strongly enhanced.

• The second mode of enhancement is by the formation of a charge-transfer complex between the surface and analyte molecule. The electronic transitions of many charge transfer complexes are in the visible, so that resonance enhancement occurs.Molecules with lone pair electrons or pi clouds show the strongest SERS. The effect was first discovered with pyridine. Other aromatic nitrogen or oxygen containing compounds, such as aromatic amines or phenols, are strongly SERS active. The effect can also been seen with other electron-rich functionalities such as carboxylic acids.The intensity of the surface plasmon resonance is dependent on many factors including the wavelength of the incident light and the morphology of the metal surface. The wavelength should match the plasma wavelength of the metal. This is about 382 nm for a 5μm silver particle, but can be as high as 600nm for larger ellipsoidal silver particles. The plasma wavelength is to the red of 650nm for copper and gold, the other two metals which show SERS at wavelengths in the 350-1000 nm region. The best morphology for surface plasmon resonance excitation is a small (<100nm) particle or an atomically rough surface.SERS is commonly employed to study monolayers of materials adsorbed on metals, including electrodes. Other popular surfaces include colloids, metal films on dielectric substrates and, recently, arrays of metal particles bound to metal or dielectric colloids through short linkages. Although SERS allows easy observation of Raman spectra from solution concentrations in the micromolar (10x-6) range,non- reproducability of quantitative measurements has in the past marred its utility for analytical purposes. However,standardization in production of SERS active media is steadilyimproving its potential in this area also.

UVRRS is a powerful tool in the molecular analysis of complex biological systems. Most biological systems absorb UV radiation and hence have the ability to offer resonance with UV Raman excitation.This results in the highly selective resonance Raman effect enabling enhancement of important biological targets such as protein or DNA. For example, excitation around 200nm enhances the Raman peaks from vibrations of amide groups; excitation around 220nm enhances peaks from certain aromatic residues.The Raman scatter from water is weak, allowing for analysis of very weak aqueous systems.

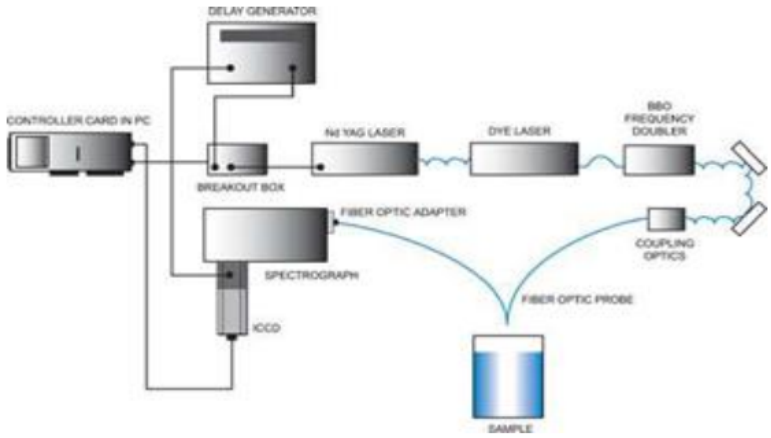

Fiber optic UVRRS configuration

Due to the selective nature of UVRRS, a tunable laser is typically required as the excitation source. Since truly tunable continuous-wave lasers are not yet available, a Nd:YAG-pumped dye laser with frequency-doubled output is one suitable UVRRS system.Depending on the dyes used, this laser setup can give almost any required UV wavelength.Intensified CCDs (ICCDs) with UV photocathodes, back-illuminated CCDs or CCDs with UV enhancing (BASF lumogen)coatings can be used as detectors for UVRRS. These detectors are used on account of their high detection efficiency and multichannel capabilities.The primary obstacle to the merging of the worlds of UVRRS and fiber-optic spectroscopy is solarization, the process by which UV radiation causes opacity of fiber-optics (even quite pure silica fibers). This opacity impairs transmission, rendering standard fiber-optics useless for UVRRS.

Vibrational Raman spectroscopy is now widely recognised as a useful technique for chemical analysis of stable species, since the technology which underpins Raman measurements has matured. Similarly, time-resolved Raman spectroscopy has also become established as an excellent method for the characterization of transient chemical species.Many of the technical advances which have reduced the cost and increased the reliability of conventional Raman systems can also be exploited in studies of transient species.

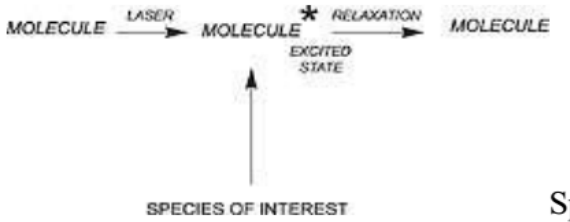

Species of Interest

Pulsed lasers are typically utilized in the study of short-lived species. A laser pulse can be supplied to a molecular system with enough energy to redistribute the electrons in a molecule causing the formation of an excited state as illustrated on the right. The Raman spectrum of this excited state molecule can be studied either using the same laser pulse or a different pulse from a second laser (single color and two-color pulsed Raman).Excited states of interest can have lifetimes, from picoseconds to milliseconds, but the majority can be studied using gating in the

order of 5ns. As the majority of excited states are generated using UV and visible lasers, photocathodes with high UV and visible Quantum Efficiencies (QE's) are typically suitable.

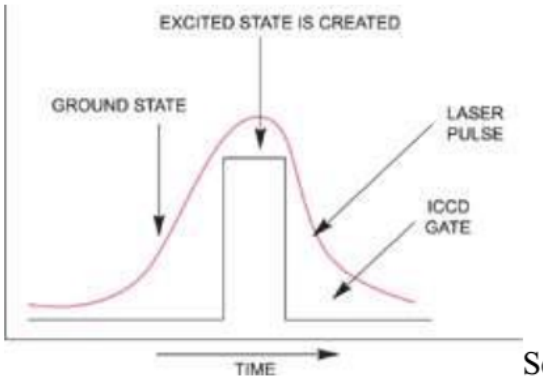

Schematic of basic pulsed excited state Raman

The simplest pulsed laser experiments are so-called single- color experiments where high irradiance laser pulses are used both to initiate the photoreaction, and then to Raman probe the transient species created within the pulse width.By opening the intensifier tube as shown on the right, only the Raman spectrum of the excited state will be recorded. This pulse/ICCD gate combination will be repeated and accumulated hundreds to thousands of times in order to achieve a good overall signal-to-noise ratio with high dynamic range.

In Time Resolved Resonance Raman (TR3) spectroscopy, pairs of laser pulses of different wavelength are used to photolyse (optically "pump") and then to Raman probe the transient species of interest.The spectral window of the spectrograph/detector is chosen so that it corresponds to the frequency range of the Raman scattering from the probe laser.

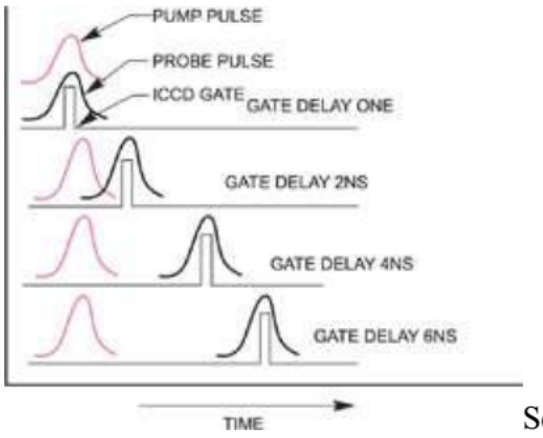

Schematic of pump-probe (two color) Raman

In Time Resolved Resonance Raman (TR3) spectroscopy, pairs of laser pulses of different wavelength are used to photolyse (optically "pump") and then to Raman probe the transient species of interest.The spectral window of the spectrograph/detector is chosen so that it corresponds to the frequency range of the Raman scattering from the probe laser.

The time evolution of the transient signal is monitored by recording a series of spectra at different delays after the photolysis event, i.e. at a series of time delays between the excitation

and probe pulses. The ICCD camera or either of the lasers can supply the trigger.A delay generator is used to controls the delays.

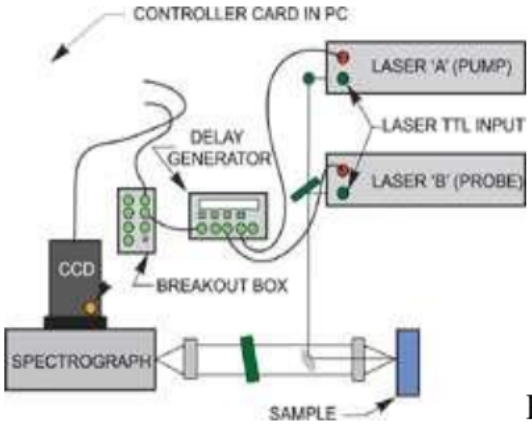

Pulsed two color Raman layout with delays under the control of a delay generator

In Raman microscopy, a research grade optical microscope is coupled to the excitation laser and the spectrometer, thus producing a platform capable of obtaining both conventional images and in addition generating Raman Spectra from sample areas approaching the diffraction limit (~1 micron). Imaging and spectroscopy can be combined to generate "Raman cubes", 3- dimensional data sets, yielding spectral information at every pixel of the 2D image.A motorized xyz microscope stage can be used to automatically record spectral files, which will constitute the basis of Raman images, Raman maps or a set of Raman spectra recorded from preselected points. Specific software routines will allow the quick and easy reconstruction of these maps.The possibility of generating two-dimensional and three-dimensional images of a sample, using various special features, is an evident advantage over either traditional spectroscopy or microscopy.

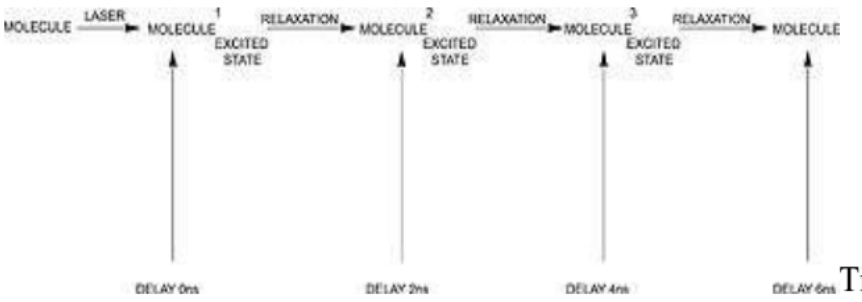

Time delay sequences

The first ever Raman "instrument" was constructed in 1928. This instrument used monochromatized sunlight as a light source and a human eye as a detector. Raman instrumentation was developed (based around arc lamps and photographic plates) and soon became very popular up until the 1950's.Since these early days, Raman instrumentation has evolved markedly. Modern instrumentation typically consists of a laser, Rayleigh filter, a few lenses, a spectrograph and a detector (typically a CCD or ICCD).

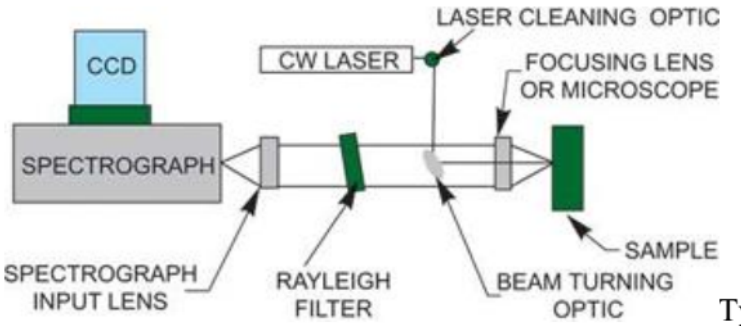

Typical Continuous Wave (CW) Raman layout

One of the major advantages of dispersive Raman is that it offers the possibility to select the optimal laser excitation wavelength to permit the recording of the best Raman information. For example, wavelengths can be selected to offer the best resonance with the sample under investigation.

One might also need to tune wavelength to avoid fluorescence and thermal emission backgrounds.Nowadays, it is possible to use laser lines from UV, (down to 200nm) up to the infrared, (1.06μm Nd:YAG laser line), from microWatts up to several Watts.

MASS SPECTROMETERY

1. The Mass Spectrometer

In order to measure the characteristics of individual molecules, a mass spectrometer converts them to ions so that they can be moved about and manipulated by external electric and magnetic fields. The three essential functions of a mass spectrometer, and the associated components, are:

1. A small sample is ionized, usually to cations by loss of an electron. **The Ion Source**
2. The ions are sorted and separated according to their mass and charge. **The Mass Analyzer**
3. The separated ions are then measured, and the results displayed on a chart. **The Detector**

Because ions are very reactive and short-lived, their formation and manipulation must be conducted in a vacuum. Atmospheric pressure is around 760 torr (mm of mercury). The pressure under which ions may be handled is roughly 10^{-5} to 10^{-8} torr (less than a billionth of an atmosphere). Each of the three tasks listed above may be accomplished in different ways. In one common procedure, ionization is effected by a high energy beam of electrons, and ion separation is achieved by accelerating and focusing the ions in a beam, which is then bent by an external magnetic field. The ions are then detected electronically and the resulting information is stored and analyzed in a computer. A mass spectrometer operating in this fashion is outlined in the following diagram. The heart of the spectrometer is the **ion source**. Here molecules of the sample (black dots) are bombarded by electrons (light blue lines) issuing from a heated filament.

This is called an **EI** (electron-impact) source. Gases and volatile liquid samples are allowed to leak into the ion source from a reservoir (as shown). Non-volatile solids and liquids may be introduced directly. Cations formed by the electron bombardment (red dots) are pushed away by a charged repeller plate (anions are attracted to it), and accelerated toward other electrodes, having slits through which the ions pass as a beam. Some of these ions fragment into smaller cations and neutral fragments. A perpendicular magnetic field deflects the ion beam in an arc whose radius is inversely proportional to the mass of each ion. Lighter ions are deflected more than heavier ions. By varying the strength of the magnetic field, ions of different mass can be focused progressively on a detector fixed at the end of a curved tube (also under a high vacuum).

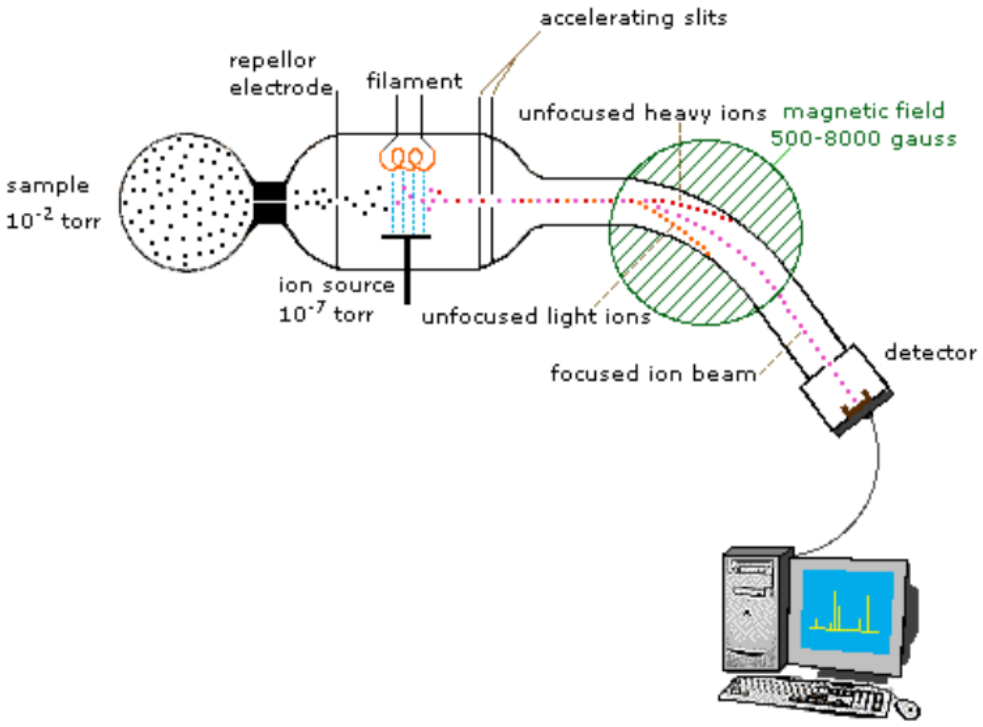

When a high energy electron collides with a molecule it often ionizes it by knocking away one of the molecular electrons (either bonding or non-bonding). This leaves behind a **molecular ion**(colored red in the following diagram). Residual energy from the collision may cause the molecular ion to fragment into neutral pieces (colored green) and smaller **fragment ions** (colored pink and orange). The molecular ion is a radical cation, but the fragment ions may either be radical cations (pink) or carbocations (orange), depending on the nature of the neutral fragment. An animated display of this ionization process will appear if you click on the ion source of the mass spectrometer diagram.

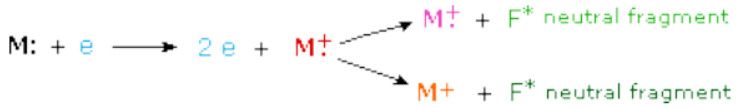

3. **The Nature of Mass Spectra**
   A mass spectrum will usually be presented as a vertical bar graph, in which each bar represents an ion having a specific mass-to-charge ratio (m/z) and the length of the bar indicates the relative abundance of the ion. The most intense ion is assigned an abundance of 100, and it is referred to as the **base peak**. Most of the ions formed in a mass spectrometer have a single charge, so the m/z value is equivalent to mass itself. Modern mass spectrometers easily distinguish (resolve) ions differing by only a single atomic mass unit (amu), and thus provide completely accurate values for the molecular mass of a compound. The highest-mass ion in a spectrum is normally considered to be the molecular ion, and lower-mass ions are fragments from the molecular ion, assuming the sample is a single pure compound.

   The following diagram displays the mass spectra of three simple gaseous compounds, carbon dioxide, propane and cyclopropane. The molecules of these compounds are similar in size, $CO_2$and C_3H_8 both have a nominal mass of 44 amu, and C_3H_6 has a mass of 42 amu. The molecular ion is the strongest ion in the spectra of CO_2 and C_3H_6, and it is moderately strong in propane. The unit mass resolution is readily apparent in these spectra (note the separation of ions having m/z=39, 40, 41 and 42 in the cyclopropane spectrum). Even though these compounds are very similar in size, it is a simple matter to identify them from their individual mass spectra. By clicking on each spectrum in turn, a partial fragmentation analysis and peak assignment will be displayed. Even with simple compounds like these, it should be noted that it is rarely possible to explain the origin of all the fragment ions in a spectrum. Also, the structure of most fragment ions is seldom known with certainty.

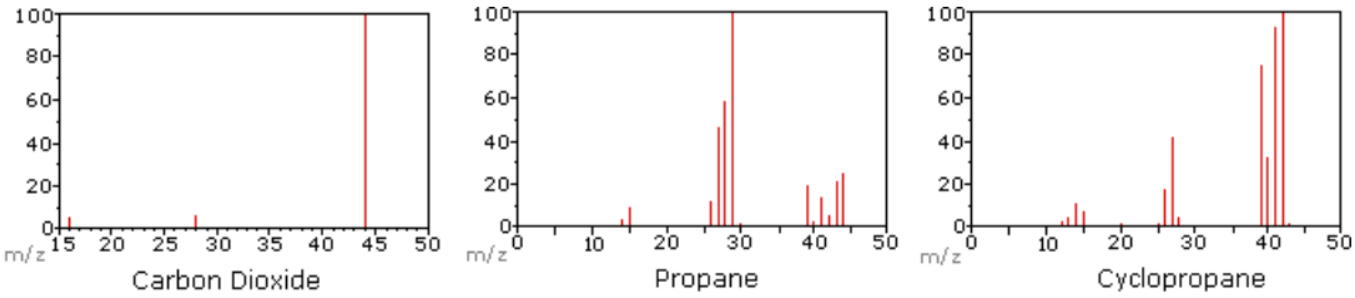

Since a molecule of carbon dioxide is composed of only three atoms, its mass spectrum is very simple. The molecular ion is also the base peak, and the only fragment ions are CO (m/z=28) and O (m/z=16). The molecular ion of propane also has m/z=44, but it is not the most abundant ion in the spectrum. Cleavage of a carbon-carbon bond gives methyl and ethyl fragments, one of which is a carbocation and the other a radical. Both distributions are observed, but the larger

ethyl cation (m/z=29) is the most abundant, possibly because its size affords greater charge dispersal. A similar bond cleavage in cyclopropane does not give two fragments, so the molecular ion is stronger than in propane, and is in fact responsible for the the base peak. Loss of a hydrogen atom, either before or after ring opening, produces the stable allyl cation (m/z=41). The third strongest ion in the spectrum has m/z=39 (C_3H_3). Its structure is uncertain, but two possibilities are shown in the diagram. The small m/z=39 ion in propane and the absence of a m/z=29 ion in cyclopropane are particularly significant in distinguishing these hydrocarbons.

Most stable organic compounds have an even number of total electrons, reflecting the fact that electrons occupy atomic and molecular orbitals in pairs. When a single electron is removed from a molecule to give an ion, the total electron count becomes an odd number, and we refer to such ions as **radical cations**. The molecular ion in a mass spectrum is always a radical cation, but the fragment ions may either be even-electron cations or odd-electron radical cations, depending on the neutral fragment lost. The simplest and most common fragmentations are bond cleavages producing a neutral radical (odd number of electrons) and a cation having an even number of electrons. A less common fragmentation, in which an even-electron neutral fragment is lost, produces an odd-electron radical cation fragment ion. Fragment ions themselves may fragment further. As a rule, odd-electron ions may fragment either to odd or even-electron ions, but even-electron ions fragment only to other even-electron ions. The masses of molecular and fragment ions also reflect the electron count, depending on the number of nitrogen atoms in the species.

Ions with no nitrogen or an even # N atoms	odd-electron ions even-number mass	even-electron ions odd-number mass
Ions having an odd # N atoms	odd-electron ions odd-number mass	even-electron ions even-number mass

This distinction is illustrated nicely by the following two examples. The unsaturated ketone, 4-methyl-3-pentene-2-one, on the left has no nitrogen so the mass of the molecular ion (m/z = 98) is an even number. Most of the fragment ions have odd-numbered masses, and therefore are even-electron cations. Diethylmethylamine, on the other hand, has one nitrogen and its molecular mass (m/z = 87) is an odd number. A majority of the fragment ions have even-numbered masses (ions at m/z = 30, 42, 56 & 58 are not labeled), and are even-electron nitrogen cations. The weak even -electron ions at m/z=15 and 29 are due to methyl and ethyl cations (no nitrogen atoms). The fragmentations leading to the chief fragment ions will be displayed by clicking on the appropriate spectrum. Repeated clicks will cycle the display.

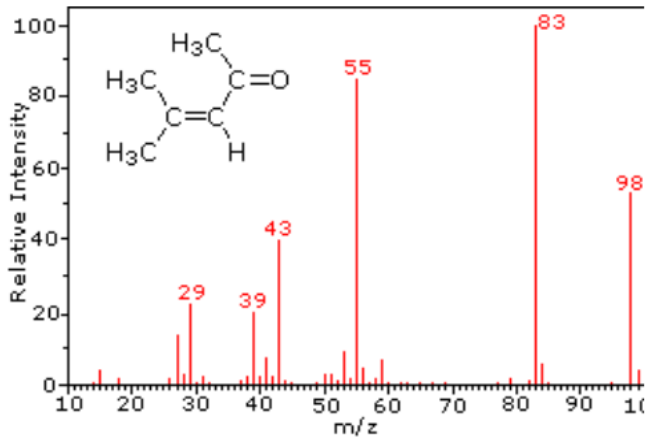

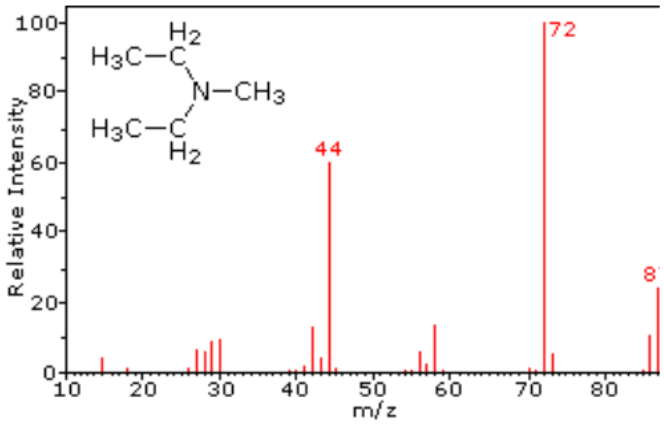

4-methyl-3-pentene-2-one **N,N-diethylmethylamine**

When non-bonded electron pairs are present in a molecule (e.g. on N or O), fragmentation pathways may sometimes be explained by assuming the missing electron is partially localized on that atom. A few such mechanisms are shown above. Bond cleavage generates a radical and a cation, and both fragments often share these roles, albeit unequally.

3. Isotopes

Since a mass spectrometer separates and detects ions of slightly different masses, it easily distinguishes different isotopes of a given element. This is manifested most dramatically for compounds containing bromine and chlorine, as illustrated by the following examples. Since molecules of bromine have only two atoms, the spectrum on the left will come as a surprise if a single atomic mass of 80 amu is assumed for Br. The five peaks in this spectrum demonstrate clearly that natural bromine consists of a nearly 50:50 mixture of isotopes having atomic masses of 79 and 81 amu respectively. Thus, the bromine molecule may be composed of two ^{79}Br atoms (mass 158 amu), two ^{81}Br atoms (mass 162 amu) or the more probable combination of ^{79}Br-^{81}Br (mass 160 amu). Fragmentation of Br_2 to a bromine cation then gives rise to equal sized ion peaks at 79 and 81 amu.

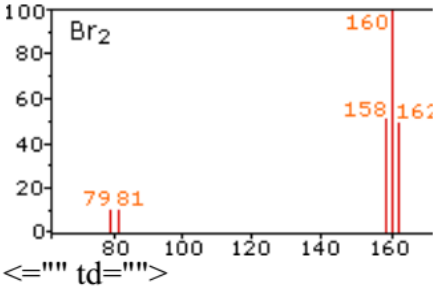

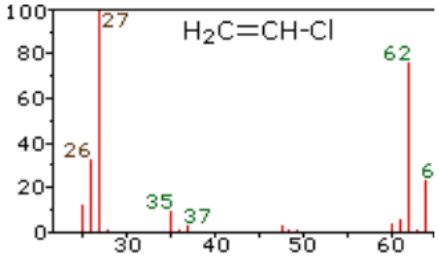

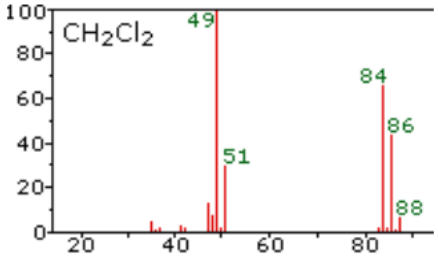

bromine **vinyl chloride** **methylene chloride**

The center and right hand spectra show that chlorine is also composed of two isotopes, the more abundant having a mass of 35 amu, and the minor isotope a mass 37 amu. The precise isotopic composition of chlorine and bromine is:

Chlorine: 75.77% ^{35}Cl and 24.23% ^{37}Cl
Bromine: 50.50% ^{79}Br and 49.50% ^{81}Br

The presence of chlorine or bromine in a molecule or ion is easily detected by noticing the intensity ratios of ions differing by 2 amu. In the case of methylene chloride, the molecular ion consists of three peaks at m/z=84, 86 & 88 amu, and their diminishing intensities may be calculated from the natural abundances given above. Loss of a chlorine atom gives two isotopic fragment ions at m/z=49 & 51amu, clearly incorporating a single chlorine atom. Fluorine and iodine, by contrast, are monoisotopic, having masses of 19 amu and 127 amu respectively. It should be noted that the presence of halogen atoms in a molecule or fragment ion does not change the odd-even mass rules given above.

To make use of a calculator that predicts the isotope clusters for different combinations of chlorine, bromine and other elements Click Here. This application was developed at Colby College.

Two other common elements having useful isotope signatures are carbon, ^{13}C is 1.1% natural abundance, and sulfur, ^{33}S and ^{34}S are 0.76% and 4.22% natural abundance respectively. For example, the small m/z=99 amu peak in the spectrum of 4-methyl-3-pentene-2-one (above) is due to the presence of a single ^{13}C atom in the molecular ion. Although less important in this respect, ^{15}N and ^{18}O also make small contributions to higher mass satellites of molecular ions incorporating these elements.

The calculator on the right may be used to calculate the isotope contributions to ion abundances 1 and 2 amu greater than the molecular ion (M). Simply enter an appropriate subscript number to the right of each symbol, leaving those elements not present blank, and press the "Calculate" button. The numbers displayed in the M+1 and M+2 boxes are relative to M being set at 100%.

4. Fragmentation Patterns

The fragmentation of molecular ions into an assortment of fragment ions is a mixed blessing. The nature of the fragments often provides a clue to the molecular structure, but if the molecular ion has a lifetime of less than a few microseconds it will not survive long enough to be observed. Without a molecular ion peak as a reference, the difficulty of interpreting a mass spectrum increases markedly. Fortunately, most organic compounds give mass spectra that include a molecular ion, and those that do not often respond successfully to the use of milder ionization conditions. Among simple organic compounds, the most stable molecular ions are those from aromatic rings, other conjugated pi-electron systems and cycloalkanes. Alcohols, ethers and highly branched alkanes generally show the greatest tendency toward fragmentation.

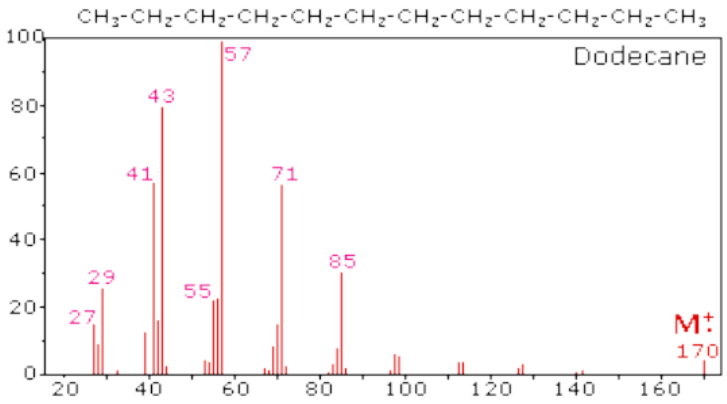

The mass spectrum of dodecane on the right illustrates the behavior of an unbranched alkane. Since there are no heteroatoms in this molecule, there are no non-bonding valence shell electrons. Consequently, the radical cation character of the molecular ion (m/z = 170) is delocalized over all the covalent bonds. Fragmentation of C-C bonds occurs because they are usually weaker than C-H bonds, and this produces a mixture of alkyl radicals and alkyl carbocations. The positive charge commonly resides on the smaller fragment, so we see a homologous series of hexyl (m/z = 85), pentyl (m/z = 71), butyl (m/z = 57), propyl (m/z = 43), ethyl (m/z = 29) and methyl (m/z = 15) cations. These are accompanied by a set of corresponding alkenyl carbocations (e.g. m/z = 55, 41 &27) formed by loss of 2 H. All of the significant fragment ions in this spectrum are even-electron ions. In most alkane spectra the propyl and butyl ions are the most abundant.

The presence of a functional group, particularly one having a heteroatom Y with non-bonding valence electrons (Y = N, O, S, X etc.), can dramatically alter the fragmentation pattern of a compound. This influence is thought to occur because of a "localization" of the radical cation component of the molecular ion on the heteroatom. After all, it is easier to remove (ionize) a non-bonding electron than one that is part of a covalent bond. By localizing the reactive moiety, certain fragmentation processes will be favored. These are summarized in the following diagram, where the green shaded box at the top displays examples of such "localized" molecular ions. The first two fragmentation paths lead to even-electron ions, and the elimination (path #3) gives an odd-electron ion. Note the use of different curved arrows to show single electron shifts compared with electron pair shifts.

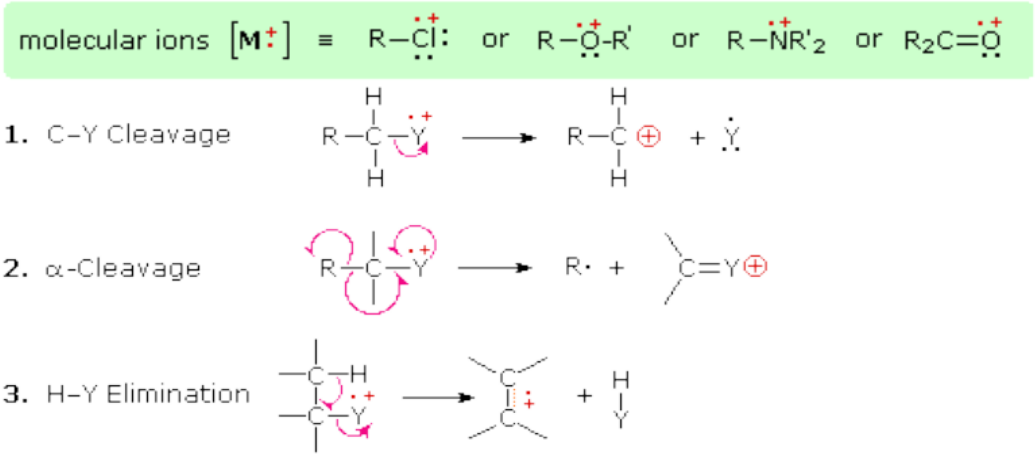

The charge distributions shown above are common, but for each cleavage process the charge may sometimes be carried by the other (neutral) species, and both fragment ions are observed. Of the three cleavage reactions described here, the alpha-cleavage is generally favored for nitrogen,

oxygen and sulfur compounds. Indeed, in the previously displayed spectra of 4-methyl-3-pentene-2-one and N,N-diethylmethylamine the major fragment ions come from alpha-cleavages. Further examples of functional group influence on fragmentation are provided by a selection of compounds that may be examined by clicking the left button below. Useful tables of common fragment ions and neutral species may be viewed by clicking the right button.

The complexity of fragmentation patterns has led to mass spectra being used as "fingerprints" for identifying compounds. Environmental pollutants, pesticide residues on food, and controlled substance identification are but a few examples of this application. Extremely small samples of an unknown substance (a microgram or less) are sufficient for such analysis. The following mass spectrum of cocaine demonstrates how a forensic laboratory might determine the nature of an unknown street drug. Even though extensive fragmentation has occurred, many of the more abundant ions (identified by magenta numbers) can be rationalized by the three mechanisms shown above. Plausible assignments may be seen by clicking on the spectrum, and it should be noted that all are even-electron ions. The m/z = 42 ion might be any or all of the following: C_3H_6, C_2H_2O or C_2H_4N. A precise assignment could be made from a high-resolution m/z value (next section).

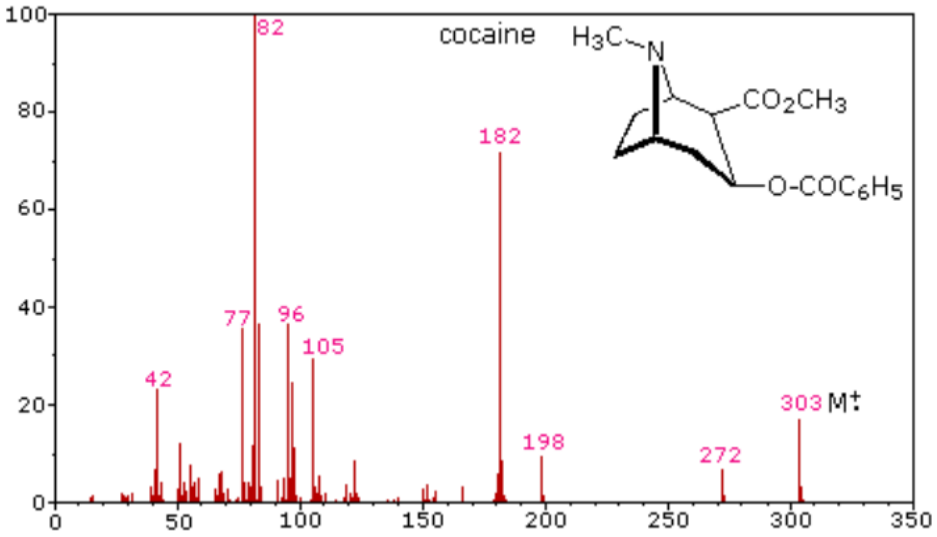

Odd-electron fragment ions are often formed by characteristic rearrangements in which stable neutral fragments are lost. Mechanisms for some of these rearrangements have been identified by following the course of isotopically labeled molecular ions. A few examples of these rearrangement mechanisms may be seen by clicking the following button.

5. High Resolution Mass Spectrometry

In assigning mass values to atoms and molecules, we have assumed integral values for isotopic masses. However, accurate measurements show that this is not strictly true. Because the strong nuclear forces that bind the components of an atomic nucleus together vary, the actual mass of a given isotope deviates from its nominal integer by a small but characteristic amount (remember $E = mc^2$). Thus, relative to ^{12}C at 12.0000, the isotopic mass of ^{16}O is 15.9949 amu (not 16) and ^{14}N is 14.0031 amu (not 14).

By designing mass spectrometers that can determine m/z values accurately to four decimal places, it is possible to distinguish different formulas having the same nominal mass. The table on the right illustrates this important feature, and a double-focusing high-resolution mass spectrometer easily distinguishes ions having these compositions. Mass spectrometry therefore not only provides a specific molecular mass value, but it may also establish the molecular formula of an unknown compound. Tables of precise mass values for any molecule or ion are available in libraries; however, the mass calculator provided below serves the same purpose. Since a given nominal mass may correspond to several molecular formulas, lists of such possibilities are especially useful when evaluating the spectrum of an unknown compound. Composition tables are available for this purpose, and a particularly useful program for calculating all possible combinations of H, C, N & O that give a specific nominal mass has been written by Jef Rozenski.

Formula	C_6H_{12}	C_5H_8O	$C_4H_8N_2$
Mass	84.0939	84.0575	84.0688

Nuclear Magnetic Resonance Spectroscopy (NMR)

1. Background

Over the past fifty years nuclear magnetic resonance spectroscopy, commonly referred to as nmr, has become the preeminent technique for determining the structure of organic compounds. Of all the spectroscopic methods, it is the only one for which a complete analysis and interpretation of the entire spectrum is normally expected. Although larger amounts of sample are needed than for mass spectroscopy, nmr is non-destructive, and with modern instruments good data may be obtained from samples weighing less than a milligram. **To be successful in using nmr as an analytical tool, it is necessary to understand the physical principles on which the methods are based**.

The nuclei of many elemental isotopes have a characteristic spin (**I**). Some nuclei have integral spins (e.g. I = 1, 2, 3 ....), some have fractional spins (e.g. I = 1/2, 3/2, 5/2 ....), and a few have no spin, I = 0 (e.g. ^{12}C, ^{16}O, ^{32}S, ...). Isotopes of particular interest and use to organic chemists are ^{1}H, ^{13}C, ^{19}F and ^{31}P, all of which have I = 1/2. Since the analysis of this spin state is fairly straightforward, our discussion of nmr will be limited to these and other I = 1/2 nuclei.

The following features lead to the nmr phenomenon:

1. A spinning charge generates a magnetic field, as shown by the animation on the right.
The resulting spin-magnet has a magnetic moment (**μ**) proportional to the spin.

2. In the presence of an external magnetic field ($\mathbf{B_0}$), two spin states exist, **+1/2** and**-1/2**.
The magnetic moment of the lower energy +1/2 state is aligned with the external field, but that of the higher energy -1/2 spin state is opposed to the external field. Note that the arrow representing the external field points North.

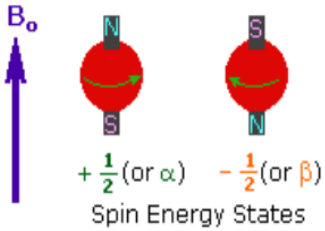

3. The difference in energy between the two spin states is dependent on the external magnetic field strength, and is always very small. The following diagram illustrates that the two spin states have the same energy when the external field is zero, but diverge as the field increases. At a field equal to B_x a formula for the energy difference is given (remember I = 1/2 and μ is the magnetic moment of the nucleus in the field).

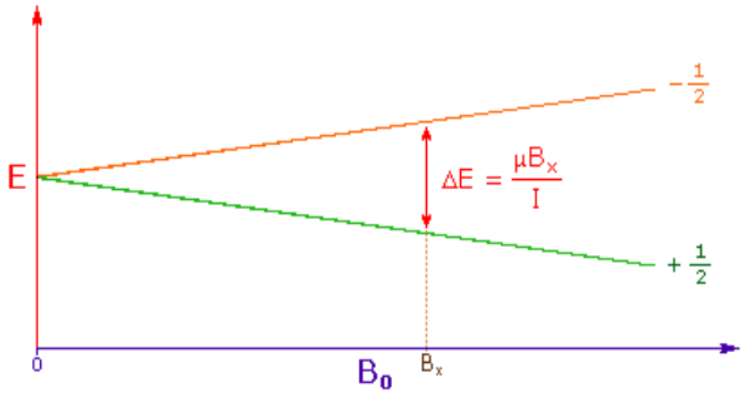

Strong magnetic fields are necessary for nmr spectroscopy. The international unit for magnetic flux is the tesla (**T**). The earth's magnetic field is not constant, but is approximately 10^{-4} T at ground level. Modern nmr spectrometers use powerful magnets having fields of 1 to 20 T. Even with these high fields, the energy difference between the two spin states is less than 0.1 cal/mole. To put this in perspective, recall that infrared transitions involve 1 to 10 kcal/mole and electronic transitions are nearly 100 time greater.
For nmr purposes, this small energy difference (ΔE) is usually given as a frequency in units of MHz (10^6 Hz), ranging from 20 to 900 Mz, depending on the magnetic field strength and the specific nucleus being studied. Irradiation of a sample with radio frequency (rf) energy corresponding exactly to the spin state separation of a specific set of nuclei will cause excitation of those nuclei in the +1/2 state to the higher -1/2 spin state. Note that this electromagnetic radiation falls in the radio and television broadcast spectrum. Nmr spectroscopy is therefore the energetically mildest probe used to examine the structure of molecules.
The nucleus of a hydrogen atom (the proton) has a magnetic moment μ = 2.7927, and has been studied more than any other nucleus. The previous diagram may be changed to display energy differences for the proton spin states (as

frequencies) by mouse clicking anywhere within it.

4. For spin 1/2 nuclei the energy difference between the two spin states at a given magnetic field strength will be proportional to their magnetic moments. For the four common nuclei noted above, the magnetic moments are: ^{1}H μ = 2.7927, ^{19}F μ = 2.6273, ^{31}P μ = 1.1305 & ^{13}C μ = 0.7022. These moments are in nuclear magnetons, which are $5.05078 \cdot 10^{-27}$ JT^{-1}. The following diagram gives the approximate frequencies that correspond to the spin state energy separations for each of these nuclei in an external magnetic field of 2.35 T. The formula in the colored box shows the direct correlation of frequency (energy difference) with magnetic moment (h = Planck's constant = $6.626069 \cdot 10^{-34}$ Js).

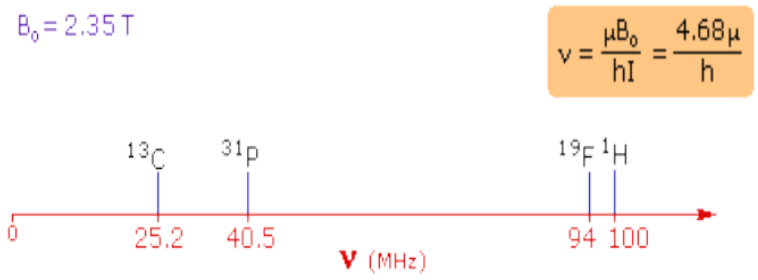

2. Proton NMR Spectroscopy

This important and well-established application of nuclear magnetic resonance will serve to illustrate some of the novel aspects of this method. To begin with, the nmr spectrometer must be tuned to a specific nucleus, in this case the proton. The actual procedure for obtaining the spectrum varies, but the simplest is referred to as the **continuous wave** (CW) method. A typical CW-spectrometer is shown in the following diagram. A solution of the sample in a uniform 5 mm glass tube is oriented between the poles of a powerful magnet, and is spun to average any magnetic field variations, as well as tube imperfections. Radio frequency radiation of appropriate energy is broadcast into the sample from an antenna coil (colored red). A receiver coil surrounds the sample tube, and emission of absorbed rf energy is monitored by dedicated electronic devices and a computer. An nmr spectrum is acquired by varying or sweeping the magnetic field over a small range while observing the rf signal from the sample. An equally effective technique is to vary the frequency of the rf radiation while holding the external field constant.

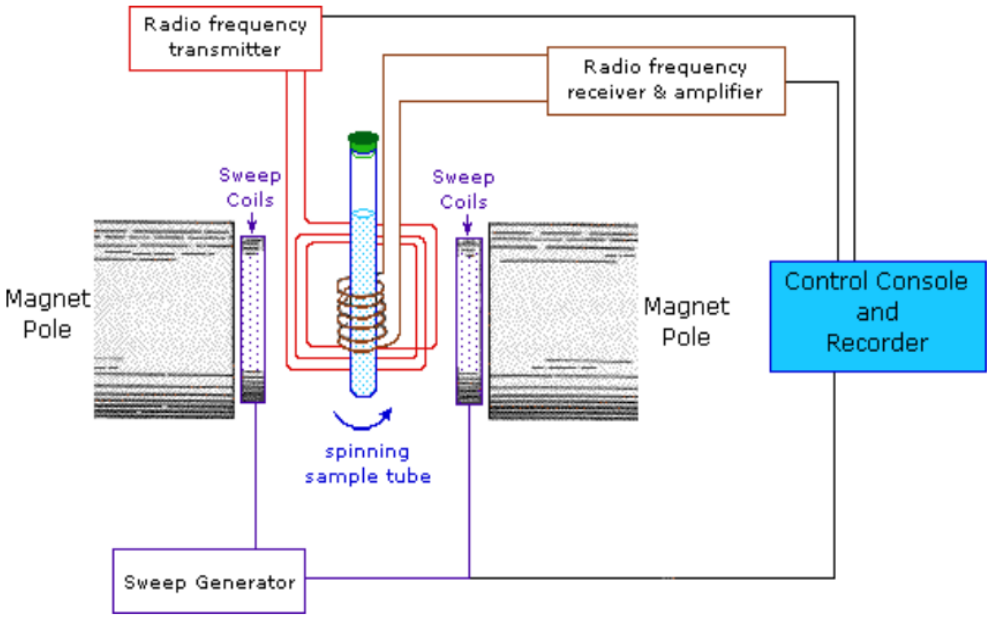

As an example, consider a sample of water in a 2.3487 T external magnetic field, irradiated by 100 MHz radiation. If the magnetic field is smoothly increased to 2.3488 T, the hydrogen nuclei of the water molecules will at some point absorb rf energy and a resonance signal will appear. An animation showing this may be activated by clicking the **Show Field Sweep** button. The field sweep will be repeated three times, and the resulting resonance trace is colored red. For visibility, the water proton signal displayed in the animation is much broader than it would be in an actual experiment.

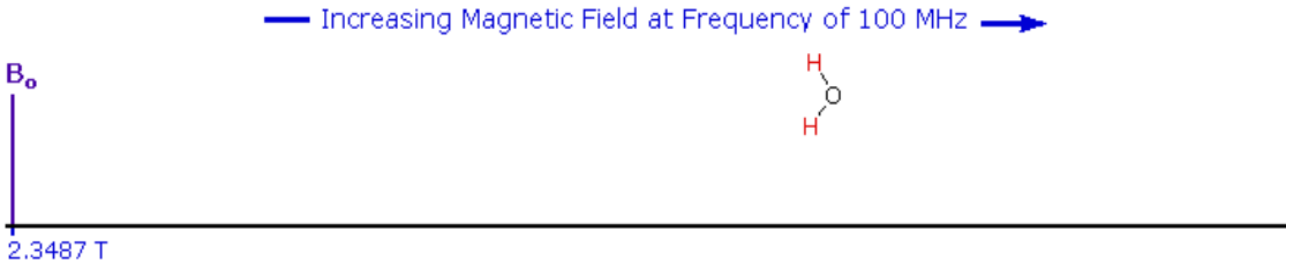

Since protons all have the same magnetic moment, we might expect all hydrogen atoms to give resonance signals at the same field / frequency values. Fortunately for chemistry applications, this is not true. By clicking the **Show Different Protons** button under the diagram, a number of representative proton signals will be displayed over the same magnetic field range. It is not possible, of course, to examine isolated protons in the spectrometer described above; but from independent measurement and calculation it has been determined that a naked proton would

resonate at a lower field strength than the nuclei of covalently bonded hydrogens. With the exception of water, chloroform and sulfuric acid, which are examined as liquids, all the other compounds are measured as gases.

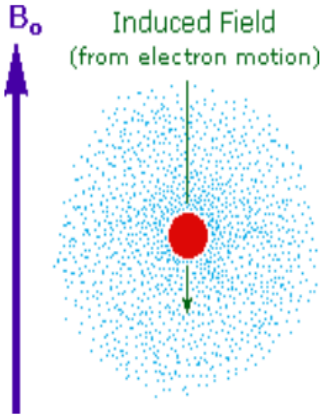

Why should the proton nuclei in different compounds behave differently in the nmr experiment ?
The answer to this question lies with the electron(s) surrounding the proton in covalent compounds and ions. Since electrons are charged particles, they move in response to the external magnetic field (B_o) so as to generate a secondary field that opposes the much stronger applied field. This secondary field **shields** the nucleus from the applied field, so B_o must be increased in order to achieve resonance (absorption of rf energy). As illustrated in the drawing on the right, B_o must be increased to compensate for the induced shielding field. In the upper diagram, those compounds that give resonance signals at the higher field side of the diagram (CH_4, HCl, HBr and HI) have proton nuclei that are more shielded than those on the lower field (left) side of the diagram. The magnetic field range displayed in the above diagram is very small compared with the actual field strength (only about 0.0042%). It is customary to refer to small increments such as this in units of **parts per million** (ppm). The difference between 2.3487 T and 2.3488 T is therefore about 42 ppm. Instead of designating a range of nmr signals in terms of magnetic field differences (as above), it is more common to use a frequency scale, even though the spectrometer may operate by sweeping the magnetic field. Using this terminology, we would find that at 2.34 T the proton signals shown above extend over a 4,200 Hz range (for a 100 MHz rf frequency, 42 ppm is 4,200 Hz). Most organic compounds exhibit proton resonances that fall within a 12 ppm range (the shaded area), and it is therefore necessary to use very sensitive and precise spectrometers to resolve structurally distinct sets of hydrogen atoms within this narrow range. In this respect it might be noted that the detection of a part-per-million difference is equivalent to detecting a 1 millimeter difference in distances of 1 kilometer.

Chemical Shift

Unlike infrared and uv-visible spectroscopy, where absorption peaks are uniquely located by a frequency or wavelength, the location of different nmr resonance signals is dependent on both the external magnetic field strength and the rf frequency. Since no two magnets will have exactly the same field, resonance frequencies will vary accordingly and an alternative method for characterizing and specifying the location of nmr signals is needed. This problem is illustrated by the eleven different compounds shown in the following diagram. Although the eleven resonance signals are distinct and well separated, an unambiguous numerical locator cannot be directly assigned to each.

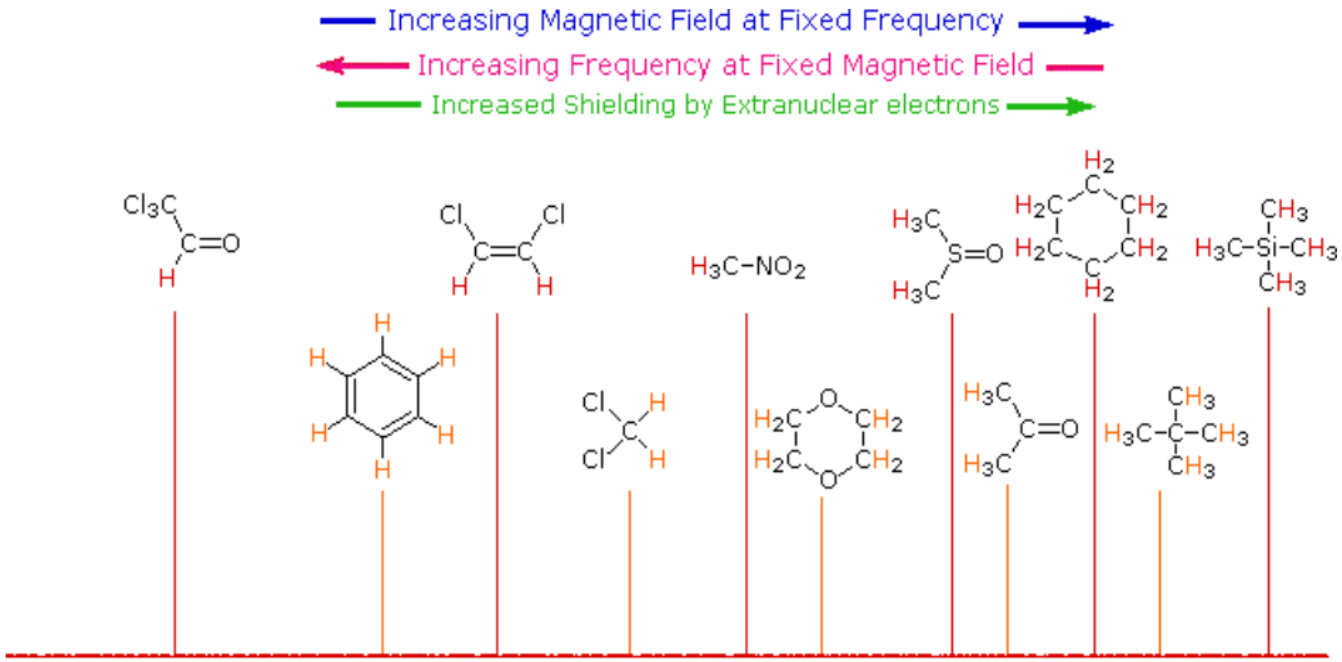

^{1}H NMR Resonance Signals for some Different Compounds

One method of solving this problem is to report the location of an nmr signal in a spectrum relative to a reference signal from a standard compound added to the sample. Such a reference standard should be chemically unreactive, and easily removed from the sample after the measurement. Also, it should give a single sharp nmr signal that does not interfere with the resonances normally observed for organic compounds. **Tetramethylsilane**, $(CH_3)_4Si$, usually referred to as **TMS**, meets all these characteristics, and has become the reference compound of choice for proton and carbon nmr.
Since the separation (or dispersion) of nmr signals is magnetic field dependent, one additional step must be taken in order to provide an unambiguous location unit. This is illustrated for the acetone, methylene chloride and benzene signals by clicking on the previous diagram. To correct these frequency differences for their field dependence, we divide them by the spectrometer frequency (100 or 500 MHz in the example), as shown in a new display by again clicking on the diagram. The resulting number would be very small, since we are dividing Hz by MHz, so it is multiplied by a million, as shown by the formula in the blue shaded box. Note that ν_{ref} is the resonant frequency of the reference signal and ν_{samp} is the frequency of the sample signal. This operation gives a locator number called the **Chemical Shift**, having units of parts-per-million (ppm), and designated by the symbol **δ** Chemical shifts for all the compounds in the original display will be presented by a third click on the diagram.

The compounds referred to above share two common characteristics:

- The hydrogen atoms in a given molecule are all structurally equivalent, averaged for fast conformational equilibria.
- The compounds are all liquids, save for neopentane which boils at 9 °C and is a liquid in an ice bath.

The first feature assures that each compound gives a single sharp resonance signal. The second allows the pure (neat) substance to be poured into a sample tube and examined in a nmr spectrometer. In order to take the nmr spectra of a solid, it is usually necessary to dissolve it in a suitable solvent. Early studies used carbon tetrachloride for this purpose, since it has no hydrogen that could introduce an interfering signal. Unfortunately, CCl_4 is a poor solvent for many polar compounds and is also toxic. Deuterium labeled compounds, such as deuterium oxide (D_2O), chloroform-d ($DCCl_3$), benzene-d_6 (C_6D_6), acetone-d_6 (CD_3COCD_3) and DMSO-d_6 (CD_3SOCD_3) are now widely used as nmr solvents. Since the deuterium isotope of hydrogen has a different magnetic moment and spin, it is invisible in a spectrometer tuned to protons.

From the previous discussion and examples we may deduce that one factor contributing to chemical shift differences in proton resonance is the **inductive effect**. If the electron density about a proton nucleus is relatively high, the induced field due to electron motions will be stronger than if the electron density is relatively low. The shielding effect in such high electron density cases will therefore be larger, and a higher external field (B_o) will be needed for the rf energy to excite the nuclear spin. Since silicon is less electronegative than carbon, the electron density about the methyl hydrogens in tetramethylsilane is expected to be greater than the electron density about the methyl hydrogens in neopentane (2,2-dimethylpropane), and the characteristic resonance signal from the silane derivative does indeed lie at a higher magnetic field. Such nuclei are said to be **shielded**. Elements that are more electronegative than carbon should exert an opposite effect (reduce the electron density); and, as the data in the following tables show, methyl groups bonded to such elements display lower field signals (they are **deshielded**). The deshielding effect of electron withdrawing groups is roughly proportional to their electronegativity, as shown by the left table. Furthermore, if more than one such group is present, the deshielding is additive (table on the right), and proton resonance is shifted even further downfield.

Proton Chemical Shifts of Methyl Derivatives

Compound	**$(CH_3)_4C$**	**$(CH_3)_3N$**	**$(CH_3)_2O$**	**CH_3F**
δ	0.9	2.1	3.2	4.1
Compound	**$(CH_3)_4Si$**	**$(CH_3)_3P$**	**$(CH_3)_2S$**	**CH_3Cl**
δ	0.0	0.9	2.1	3.0

Proton Chemical Shifts (ppm)

Cpd. / Sub.	**X=Cl**	**X=Br**	**X=I**	**X=OR**	**X=SR**
CH_3X	3.0	2.7	2.1	3.1	2.1
CH_2X_2	5.3	5.0	3.9	4.4	3.7
CHX_3	7.3	6.8	4.9	5.0	

The general distribution of proton chemical shifts associated with different functional groups is summarized in the following chart. Bear in mind that these ranges are approximate, and may not encompass all compounds of a given class. Note also that the ranges specified for OH and NH protons (colored orange) are wider than those for most CH protons. This is due to hydrogen bonding variations at different sample concentrations.

Proton Chemical Shift Ranges*

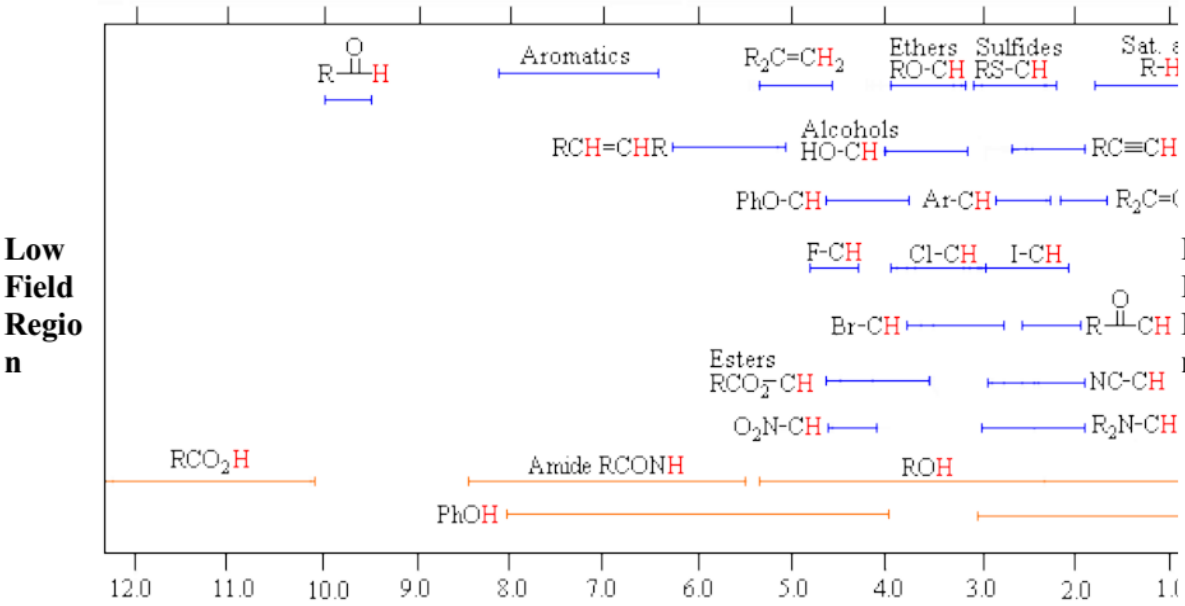

* For samples in $CDCl_3$ solution. The δ scale is relative to TMS at δ = 0.

To make use of a calculator that predicts aliphatic proton chemical shifts Click Here. This application was developed at Colby College.

Signal Strength

The magnitude or intensity of nmr resonance signals is displayed along the vertical axis of a spectrum, and is proportional to the molar concentration of the sample. Thus, a small or dilute sample will give a weak signal, and doubling or tripling the sample concentration increases the signal strength proportionally. If we take the nmr spectrum of equal molar amounts of benzene and cyclohexane in carbon tetrachloride solution, the resonance signal from cyclohexane will be twice as intense as that from benzene because cyclohexane has twice as many hydrogens per molecule. This is an important relationship when samples incorporating two or more different sets of hydrogen atoms are examined, since it allows the ratio of hydrogen atoms in each distinct set to be determined. To this end it is necessary to measure the relative strength as well as the chemical shift of the resonance signals that comprise an nmr spectrum. Two common methods of displaying the integrated intensities associated with a spectrum are illustrated by the following examples. In the three spectra in the top row, a horizontal integrator trace (light green) rises as it crosses each signal by a distance proportional to the signal strength. Alternatively, an arbitrary number, selected by the instrument's computer to reflect the signal strength, is printed below each resonance peak, as shown in the three spectra in the lower row. From the relative intensities shown here, together with the previously noted chemical shift correlations, the reader should be able to assign the signals in these spectra to the set of hydrogens that generates each. If you click on one of the spectrum signals (colored red) or on hydrogen atom(s) in the structural formulas the spectrum will be enlarged and the relationship will be colored blue. **Hint:** When evaluating relative signal strengths, it is useful to set the smallest integration to unity and convert the other values proportionally.

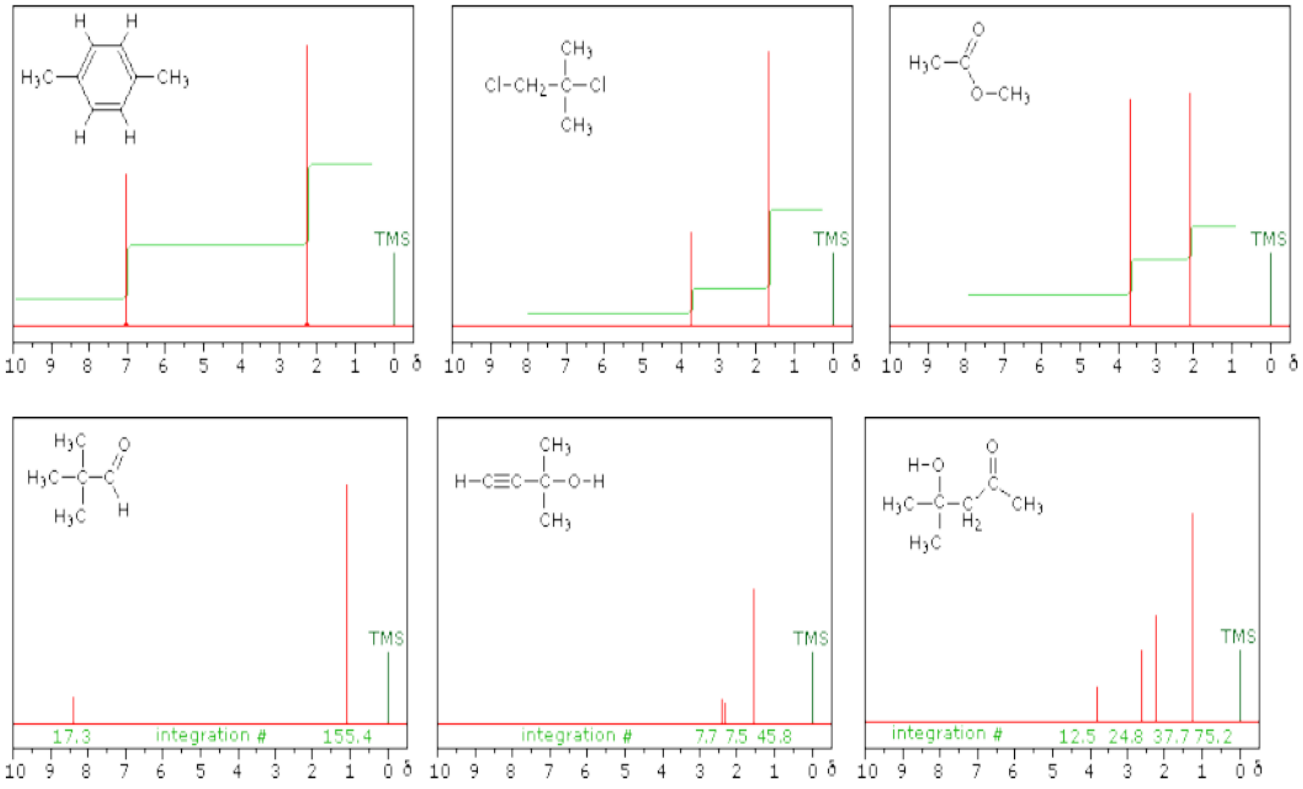

Hydroxyl Proton Exchange and the Influence of Hydrogen Bonding

The last two compounds in the lower row are alcohols. The OH proton signal is seen at 2.37 δ in 2-methyl-3-butyne-2-ol, and at 3.87 δ in 4-hydroxy-4-methyl-2-pentanone, illustrating the wide range over which this chemical shift may be found. A six-membered ring intramolecular hydrogen bond in the latter compound is in part responsible for its low field shift, and will be shown by clicking on the hydroxyl proton. We can take advantage of rapid OH exchange with the deuterium of heavy water to assign hydroxyl proton resonance signals . As shown in the following equation, this removes the hydroxyl proton from the sample and its resonance signal in the nmr spectrum disappears. Experimentally, one simply adds a drop of heavy water to a chloroform-d solution of the compound and runs the spectrum again. The result of this exchange is displayed below.

$$\text{R-O-H} + D_2O \rightleftharpoons \text{R-O-D} + \text{D-O-H}$$

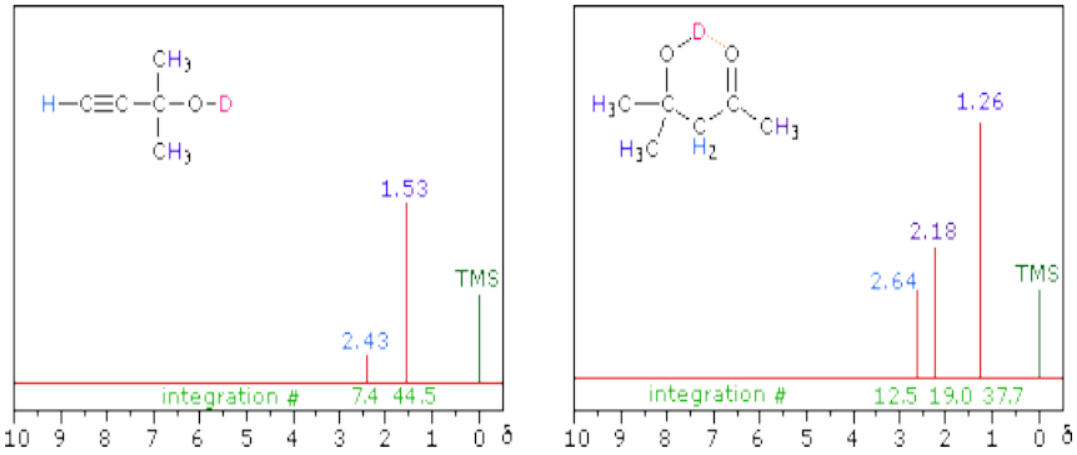

Hydrogen bonding shifts the resonance signal of a proton to lower field (higher frequency

i). Numerous experimental observations support this statement, and a few of these will be described here.

i) The chemical shift of the hydroxyl hydrogen of an alcohol varies with concentration. Very dilute solutions of 2-methyl-2-propanol, $(CH_3)_3COH$, in carbon tetrachloride solution display a hydroxyl resonance signal having a relatively high-field chemical shift (< 1.0 δ). In concentrated solution this signal shifts to a lower field, usually near 2.5 δ.

ii) The more acidic hydroxyl group of phenol generates a lower-field resonance signal, which shows a similar concentration dependence to that of alcohols. OH resonance signals for different percent concentrations of phenol in chloroform-d are shown in the following diagram (C-H signals are not shown).

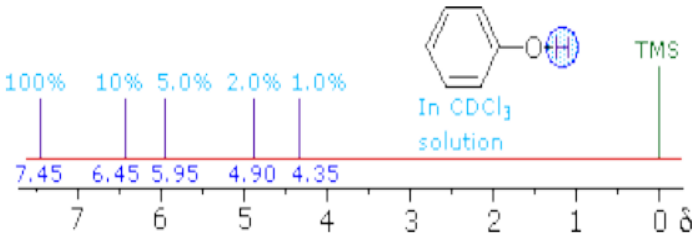

iii) Because of their favored hydrogen-bonded dimeric association, the hydroxyl proton of carboxylic acids displays a resonance signal significantly down-field of other functions. For a typical acid it appears from 10.0 to 13.0 δ and is often broader than other signals. The spectra shown below for chloroacetic acid (left) and 3,5-dimethylbenzoic acid (right) are examples.

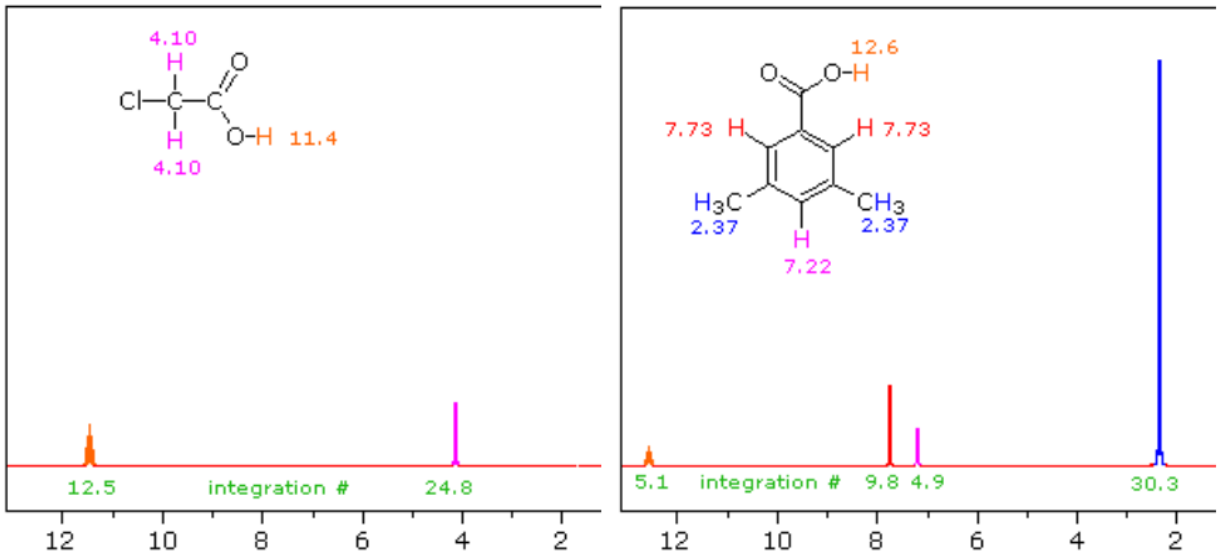

iv) Intramolecular hydrogen bonds, especially those defining a six-membered ring, generally display a very low-field proton resonance. The case of 4-hydroxypent-3-ene-2-one (the enol tautomer of 2,4-pentanedione) not only illustrates this characteristic, but also provides an instructive example of the sensitivity of the nmr experiment to dynamic change. In the nmr spectrum of the pure liquid, sharp signals from both the keto and enol tautomers are seen, their mole ratio being 4 **:** 21 (keto tautomer signals are colored purple). Chemical shift assignments for these signals are shown in the shaded box above the spectrum. The chemical shift of the hydrogen-bonded hydroxyl proton is δ 14.5, exceptionally downfield. We conclude, therefore, that the rate at which these tautomers interconvert is slow compared with the inherent time scale of nmr spectroscopy.

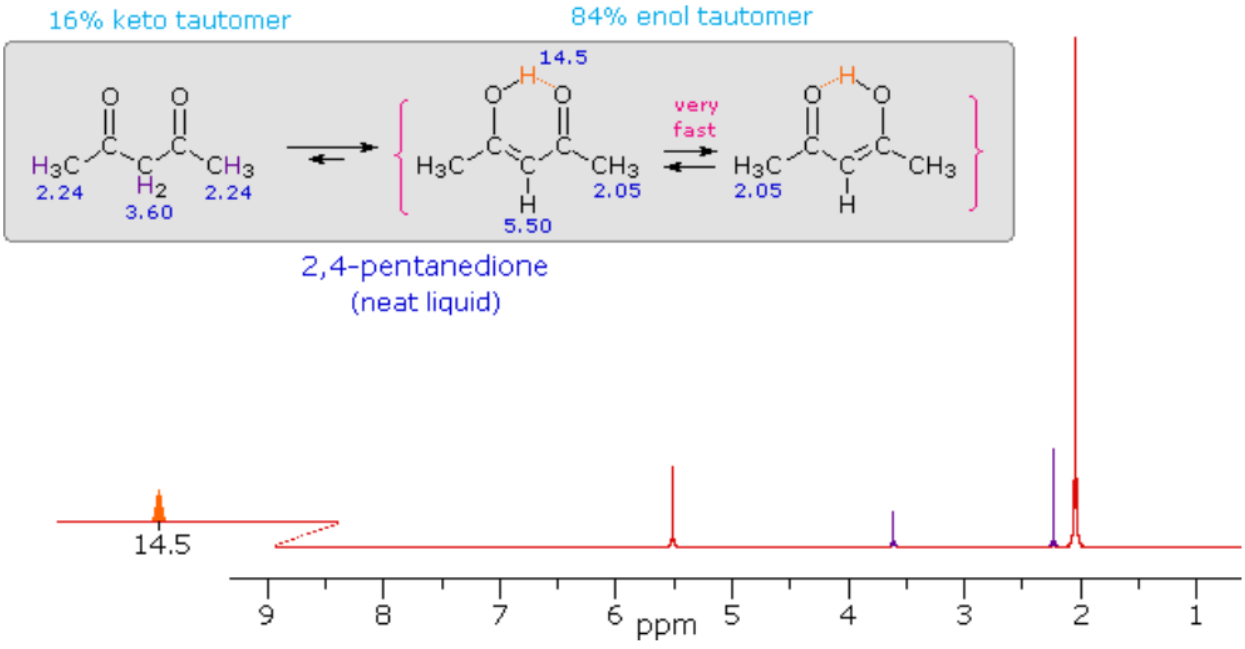

Two structurally equivalent structures may be drawn for the enol tautomer (in magenta brackets).

If these enols were slow to interconvert, we would expect to see two methyl resonance signals associated with each, one from the allylic methyl and one from the methyl ketone. Since only one strong methyl signal is observed, we must conclude that the interconversion of the enols is very fast-so fast that the nmr experiment detects only a single time-averaged methyl group (50% α-keto and 50% allyl).

Although hydroxyl protons have been the focus of this discussion, it should be noted that corresponding N-H groups in amines and amides also exhibit hydrogen bonding nmr shifts, although to a lesser degree. Furthermore, OH and NH groups can undergo rapid proton exchange with each other; so if two or more such groups are present in a molecule, the nmr spectrum will show a single signal at an average chemical shift. For example, 2-hydroxy-2-methylpropanoic acid, $(CH_3)_2C(OH)CO_2H$, displays a strong methyl signal at δ 1.5 and a 1/3 weaker and broader OH signal at δ 7.3 ppm. Note that the average of the expected carboxylic acid signal (ca. 12) and the alcohol signal (ca. 2) is 7. Rapid exchange of these hydrogens with heavy water, as noted above, would cause the low field signal to disappear.